



**HAL**  
open science

# Estimating daily climatological normals in a changing climate

Alix Rigal, Jean-Marc Azaïs, Aurélien Ribes

► **To cite this version:**

Alix Rigal, Jean-Marc Azaïs, Aurélien Ribes. Estimating daily climatological normals in a changing climate. *Climate Dynamics*, In press, 10.1007/s00382-018-4584-6 . hal-01980565

**HAL Id: hal-01980565**

**<https://hal.science/hal-01980565v1>**

Submitted on 5 Feb 2019

**HAL** is a multi-disciplinary open access archive for the deposit and dissemination of scientific research documents, whether they are published or not. The documents may come from teaching and research institutions in France or abroad, or from public or private research centers.

L'archive ouverte pluridisciplinaire **HAL**, est destinée au dépôt et à la diffusion de documents scientifiques de niveau recherche, publiés ou non, émanant des établissements d'enseignement et de recherche français ou étrangers, des laboratoires publics ou privés.

1 **Estimating daily climatological normals in a**  
2 **changing climate**

3 **Alix Rigal · Jean-Marc Azaïs · Aurélien**  
4 **Ribes**

5  
6 Received: 06 April 2018 / Accepted: date

7 **Abstract** Climatological normals are widely used baselines for the descrip-  
8 tion and the characterization of a given meteorological situation. The World  
9 Meteorological Organization (WMO) standard recommends estimating clima-  
10 tological normals as the average of observations over a 30-year period. This  
11 approach may lead to strongly biased normals in a changing climate. Here we  
12 propose a new method with which to estimate daily climatological normals in  
13 a non-stationary climate. Our statistical framework relies on the assumption  
14 that the response to climate change is smooth over time, and on a decompo-  
15 sition of the response inspired by the pattern scaling assumption. Estimation  
16 is carried out using smoothing splines techniques, with a careful examination  
17 of the selection of smoothing parameters. The new method is compared, in  
18 a predictive sense and in a perfect model framework, to previously proposed  
19 alternatives such as the WMO standard (reset either on a decadal or an-  
20 nual basis), averages over shorter periods, and hinge fits. Results show that  
21 our technique outperforms all alternatives considered. They confirm that pre-  
22 viously proposed techniques are substantially biased – biases are typically as  
23 large as a few tenth to more than 1 degree by the end of the century – while our  
24 method is not. We argue that such “climate change corrected” normals might  
25 be very useful for climate monitoring, and that weather services could consider  
26 using two different sets of normals (i.e. both stationary and non-stationary)  
27 for different purposes.

---

Also funded by Météo France.

Alix Rigal  
CNRM, UMR3589, Météo-France and CNRS, Toulouse, France  
E-mail: alix.rigal@meteo.fr

Jean-Marc Azaïs  
Institut de Mathématiques, Université Paul Sabatier (member of the federal University  
"Université de Toulouse"), 31062 Toulouse, cedex 09 France

Aurélien Ribes  
CNRM, UMR3589, Météo-France and CNRS, Toulouse, France

28 **Keywords** daily climate normals · unbiased estimate · normals accounting  
29 for climate change · Smoothing splines

## 30 1 Introduction

31 Climatological normals are widely used baselines which describe and charac-  
32 terise a given meteorological situation. On the news, weather forecasts com-  
33 monly refer to normals in order to compare a weather or seasonal forecast to  
34 its expectation. Retrospective climate monitoring also typically involves such  
35 a comparison. Climate normals are primarily meant to describe the mean sea-  
36 sonal cycle in standard meteorological variables such as temperature or pre-  
37 cipitation. In the most common estimation techniques, normals are assumed  
38 to be stationary, i.e. the drift related to anthropogenic climate change is ne-  
39 glected, potentially leading to inaccurate or biased estimates. One issue with  
40 this approach is that, as pointed out by Arguez and Vose (2011): “climate  
41 normals are calculated retrospectively, but are often utilized prospectively”.  
42 For instance, when they are compared to weather forecasts, it is assumed that  
43 normals provide an estimation of the expected weather to date. Neglecting  
44 on-going warming can prevent this.

45 For example, the current recommendation of the World Meteorological Or-  
46 ganization (WMO) for the calculation of climatological normals, known as the  
47 Climatological Standard Normals, is to compute an average over a 30-year  
48 period (World Meteorological Organization, 2007; Baddour, 2011)  
49 (ref to [http://www.wmo.int/pages/prog/wcp/wcdmp/GCDS\\_1.php](http://www.wmo.int/pages/prog/wcp/wcdmp/GCDS_1.php)). These  
50 normals are supposed to be updated every 30 years, with the current refer-  
51 ence period being 1961-1990. Following these recommendations, the next  
52 generation of climatological normals would be available in 2021, based on the  
53 1991-2020 average.

54 Several studies pointed out the limitation of such normals and their in-  
55 accuracy in a non-stationary climate (e.g Scherrer, Appenzeller, and Liniger  
56 (2006); Krakauer and Devineni (2015)). WMO itself advocated for a more  
57 frequent revision of climate normals, through updates every 10 years but  
58 still averaging over a 30-year period (Wright, 2014). This change was in-  
59 tended to reduce the bias, with a careful discussion of pros and cons in or-  
60 der to define a dual standard for normals. Other authors, e.g. Livezey, Vin-  
61 nikov, Timofeyeva, Tinker, and van den Dool (2007); Wilks (2013); Wilks  
62 and Livezey (2013), proposed alternative methods for deriving climatological  
63 normals and assessed these methods across the US. Optimal Climatological  
64 Normals (OCNs) are averages calculated over periods shorter than 30-years.  
65 The length of the averaging period is then selected to maximize the accuracy  
66 of the estimation – the authors typically considered 15-year means for tem-  
67 peratures across the US. Hinge fits are break-point statistical models where  
68 the climatological mean is expected to be constant before a given date, and  
69 linearly growing after that date. Authors cited above suggest that 1975 is a  
70 good choice for the break point over the US. Some national meteorological

71 services already use these alternative estimation techniques operationally (ref  
72 to <https://www.ncdc.noaa.gov/normalsPDFaccess/>).

73 Another important feature of climatological normals is their time-resolution.  
74 Most normals are calculated on a monthly time-scale. However, for specific  
75 applications, the estimation of daily normals is required (Arguez, Vose, and  
76 Dissen, 2013). A few techniques have been proposed and /or are routinely used  
77 to translate monthly into daily values (Arguez and Applequist, 2013; Arguez,  
78 Applequist, Vose, Durre, Squires, and Yin, 2011; Arguez, Durre, Applequist,  
79 Vose, Squires, Yin, Heim, and Owen, 2012). Another option is to estimate  
80 daily normals directly from raw data, assuming some type of regularity in the  
81 seasonal variations (i.e. normals do not vary much from one day to the next).  
82 Doing this in a non-stationary context will require smoothness both in the sea-  
83 sonal cycle and the climate change components. This is the method employed  
84 in this manuscript.

85 In this paper, we assess the accuracy of previously proposed techniques for  
86 the estimating of climatological normals. We outline their limitations if applied  
87 in the course of the 21st century. We then introduce a new approach for the  
88 overcoming of these issues. With this approach, the drift related to climate  
89 change on the seasonal component is estimated, leading to daily estimates.  
90 All evaluations are made in a predictive sense, i.e. assessing whether normals  
91 calculated in the (recent) past provide a reliable estimation of current to near-  
92 future climates.

93 The manuscript is organized as follows. After presenting the dataset in  
94 Section 2 we elaborate on the methods used to estimate climatological nor-  
95 mals, then introduce our new method. The predictive skills of the various  
96 techniques considered are assessed and discussed in Section 4. This is followed  
97 by a discussion along with some concluding remarks in the last section.

## 98 **2 Data & existing methods**

### 99 **2.1 Data**

100 In order to assess the accuracy of various techniques for estimating climato-  
101 logical normals during the 21st century – a period over which observations are  
102 not available – we use series of daily and annual mean temperatures. These  
103 are simulated by an ensemble of climate models from the Coupled Model In-  
104 tercomparison Project Phase 5 (CMIP5) as realistic realizations of future ob-  
105 servations. Estimation techniques are therefore compared in a perfect model  
106 framework (see more details in Section 4).

107 More specifically, we focus on four locations which are meant to be repre-  
108 sentative of a wide range of climates: Bengaluru (India) in the tropics, Alert  
109 (Canadian Arctic Archipelago) in high-latitude, Paris (France) and San Fran-  
110 cisco (California, USA) in mid-latitude regions. Twenty one CMIP5 models  
111 were selected for the daily mean temperature and sixty for the annual mean  
112 temperature (see Appendix A for a detailed list of models).

113 The considered time-series cover a period of 238 years from 1862 to 2099.  
 114 They consist of the concatenation of two types of experiments:

- 115 – historical runs (driven by observed radiative forcings) covering the period  
 116 1862-2005,
- 117 – RCP8.5 scenario (Representative Concentration Pathways 8.5, correspond-  
 118 ing to a high increase in greenhouse gas emissions during the 21st) simu-  
 119 lations covering the remaining of the 21<sup>St</sup> century (2006-2100).

120 The choice of a RCP8.5 scenario involves a strong climate change signal in the  
 121 coming decades, but results obtained with this scenario are expected to hold  
 122 at least qualitatively with more moderated alternatives.

123 It must be noted that for daily calculations, all the 29<sup>Th</sup> February were  
 124 removed to facilitate processing. Also, extensions to other climate variables,  
 125 such as precipitation, are beyond the scope of this paper.

## 126 2.2 Previously introduced methods considered within this study

127 Here we review methods proposed by various authors in order to estimate cli-  
 128 matological normals. Some of these techniques have been introduced in order  
 129 to cope with climate change, and/or build upon the standard WMO recom-  
 130 mendation. First we explain how these methods can be used to estimate annual  
 131 normals, then we discuss how they can be extended to the daily timescale. This  
 132 list of techniques is not meant to be exhaustive, but instead representative of  
 133 what has been proposed in the literature.

### 134 – 2.2.1 *WMO standard*

135 The WMO recommendation is to calculate climatological normals as a  
 136 simple average over a 30-year period composed of 3 full decades:

$$137 \quad WMO(D+k) = \frac{1}{30} \sum_{i=D-29}^D T_i, \quad (1)$$

138 where  $D+k$  is the current year,  $D$  is the current decade (e.g 2010),  $k \in$   
 139  $\llbracket 1, 10 \rrbracket$  denotes the year within the decade,  $T_i$  is the mean temperature (or  
 140 any other meteorological variable) of year  $i$ . This calculation is updated  
 141 every 10 years which means that, after a decade is completed, the estimated  
 142 normals are valid and can be used for the subsequent 10 years (as denoted  
 by  $D+k$  in (1)).

### 143 – 2.2.2 *WMO reset*

144 As a first very simple alternative, the same calculation can be made and  
 145 updated every year (instead of every decade), leading to

$$146 \quad WMO(y) = \frac{1}{30} \sum_{i=y-30}^{y-1} T_i, \quad (2)$$

146 where  $y$  is the current year. This will be referred to as WMO reset in  
 147 the following, and is expected to be less biased than WMO in a changing  
 148 climate thanks to the more frequent update.

149 – *2.2.3 Optimal Climate Normals (OCN)*

150 Huang, van den Dool, and Barnston (1996); Wilks (2013); Wilks and  
 151 Livezey (2013) argued that averaging over a 30-year period was non-optimal  
 152 (too long) in a climate change context, and suggested tuning the length of  
 153 the averaging period to improve the accuracy of the estimate. They sug-  
 154 gested that averaging over the most recent 15 years was a good compromise  
 155 for temperature normals. As follows, OCN therefore designates a 15-year  
 156 average:

$$OCN(D+k) = \frac{1}{15} \sum_{i=D-14}^D T_i, \quad (3)$$

157 with  $k \in \llbracket 1, 10 \rrbracket$ . As for WMO, this average can be updated every 10 years  
 158 (as assumed in the following), or every year. In the following, this 15-year  
 159 average will be used as a benchmark for other operational normals using  
 160 the mean of a different number of years.

161 – *2.2.4 Hinge fit*

162 In order to account for non-stationary climates, other authors proposed  
 163 the use of a statistical model allowing for a trend in the estimation of  
 164 climate normals. Among these, the most popular technique is the hinge  
 165 fit (Livezey et al, 2007; Wilks and Livezey, 2013). This is a simple break-  
 166 point model where the normals are assumed to be constant (i.e. non time-  
 167 dependent) up to a given date, then linearly moving with time. The date of  
 168 the break-point needs to be selected carefully – Livezey et al (2007), Wilks  
 169 and Livezey (2013) suggested that 1975 was an appropriate choice for the  
 170 continental US and this is the value used in this paper.

$$Hinge(D+k) = \beta_0 + \beta_1 I_{1975}(D+k), \quad (4)$$

171 where  $I(x) = 0$  if  $x \leq 1975$  and  $I(x) = x - 1975$  if  $x > 1975$ . The coeffi-  
 172 cients  $\beta_0$  and  $\beta_1$  are estimated from the full observational record available  
 173 up to year  $D$  (i.e. not restricted to a 30-year period) using simple linear  
 174 regression. Again this type of estimate could be updated each decade or  
 175 year.

176 – *2.2.5 Hinge fit reset*

177 The same calculation can be made and updated every year instead of every  
 178 decade, leading to

$$Hinge(y) = \beta_0 + \beta_1 I_{1975}(y), \quad (5)$$

179 The coefficients  $\beta_0$  and  $\beta_1$  are estimated from the full observational record  
 180 available up to year  $y-1$  using simple linear regression. This will be referred  
 181 to as Hinge fit reset in the following.

### 182 2.2.6 From annual to daily normals

183 All of the techniques listed above can be used to derive daily (instead of  
 184 yearly or even monthly) normals. This requires an additional procedure first  
 185 introduced by Arguez and Appleyard (2013) and consisting of an expansion  
 186 in a Fourier basis. This technique is described below using the WMO estimate  
 187 as an example, but it can be applied to any other normal estimator, including  
 188 the OCN and Hinge methods introduced above. Firstly, we compute normals  
 189 for each single day within a year, i.e.

$$WMO_{raw}(D+k, d) = \frac{1}{30} \sum_{i=D-29}^D T_{i,d}, \quad (6)$$

190 where  $d \in \llbracket 1, 365 \rrbracket$  represents the day, while other notations are consistent with  
 191 (1). These daily values are then fitted onto the thirteen first elements of the  
 192 Fourier basis. Equivalently, we estimate the linear coefficients  $\alpha_i, \beta_i$  involved  
 193 in the statistical model

$$WMO_{raw}(D+k, d) = \alpha_0 + \sum_{k=1}^6 \left( \alpha_k \cos\left(\frac{2k\pi}{365}d\right) + \beta_k \sin\left(\frac{2k\pi}{365}d\right) \right) + \varepsilon_d. \quad (7)$$

194 Finally the estimated daily normals  $WMO_{day}$  for year  $D+k$  and day  $d$  are

$$WMO_{day}(D+k, d) = \hat{\alpha}_0 + \sum_{k=1}^6 \left( \hat{\alpha}_k \cos\left(\frac{2k\pi}{365}d\right) + \hat{\beta}_k \sin\left(\frac{2k\pi}{365}d\right) \right), \quad (8)$$

195 where  $\hat{\alpha}_i, \hat{\beta}_i$  are the estimated regression coefficients. Through projection onto  
 196 a Fourier basis, this technique ensures regularity in the estimated annual cycle.

## 197 3 New Method

198 All methods described above could be criticized for a certain lack of flexibil-  
 199 ity (e.g. Krakauer (2012)). Indeed, climate is either assumed to be stationary  
 200 locally (computing averages) or moving linearly over time, with the linearity  
 201 holding over a relatively long period of time, from 1975 onwards (hinge fit).  
 202 In this section, we introduce an alternative method for computing climatolog-  
 203 ical normals, which is somewhat more flexible for its being based on spline  
 204 smoothing. Obviously, the increase in flexibility is at the cost of an increase in  
 205 the variance of the estimator – this will be discussed through the investigation  
 206 of the overall performance of our approach in subsequent sections.

### 3.1 Statistical framework

The general statistical model considered is inspired by and adapted from Azaïs and Ribes (2016). Let  $T_{y,d}$  be the mean (i.e. statistical expectation of) temperature of day  $d$  in year  $y$ . Our statistical model assumes that the following decomposition holds:

$$T_{d,y} = f(d) + g(y)h(d) + \varepsilon_{d,y}, \quad d \in \llbracket 1, 365 \rrbracket, y \in \llbracket 1, n \rrbracket, \quad (9)$$

where:

- $f(), g(), h()$  are smooth functions ( $f(d), g(y), h(d)$  being their trace on integer values),
- $f(), h()$  are, additionally, periodic functions with period 365,
- $\varepsilon$  is assumed to be Gaussian white noise with unknown variance  $\sigma^2$ .

In addition we impose the constraints  $\sum_{y=1}^n g(y) = 0$  and  $\sum_{d=1}^{365} h(y) = 1$  in order to ensure model identifiability (i.e. to avoid any possible confusion between the terms  $f$  and  $gh$ ). Note that another system of constraints is possible in order to facilitate interpretation (see Appendix B).

This statical model can be interpreted as follows.  $f(d)$  represents a stationary seasonal cycle, which would be observed if the climate was stationary and the effect of climate change is described by the term  $g(y)h(d)$ . The key assumption is that this climate change response can be factorized into one component which describes how the shape of a seasonal cycle changes,  $h(d)$ , and another one which describes the variation of the magnitude of this change with time, in the long-term,  $g(y)$ .

This type of decomposition is an adaptation of the *pattern scaling* assumption (Mitchell, 2003; Tebaldi and Arblaster, 2014; Geoffroy and Saint-Martin, 2014) in a slightly different setup. Under *pattern scaling*, it is assumed that the spatial distribution of climate change does not vary with time – only the amplitude of the change does. It is thus possible to decompose climate change as the product between one spatial function, and one temporal function. In the present paper, the spatial component is replaced by the seasonal cycle. In both cases, the assumption can be thought of as a Taylor approximation of order one, which is valid as long as the change is small enough. This factorization assumption is obviously one of consequence but has already proven its descriptive capabilities on hourly surface air temperature observations (Vinnikov, Robock, Grody, and Basist, 2004). Its primary interest comes from the induced reduction in the model’s complexity: estimating two univariate functions  $g$  and  $h$  is much easier than estimating a bivariate function (say  $c(y, d)$ ). Its introduction therefore allows us to better constrain the estimation of the climate change component. Additionally, model (9) proved a very good capability across the entire time series considered and it can be at least partially validated by examining goodness-of-fit to model (9), as discussed below.

An illustration of this model and the typical outputs it can produce, is shown in Figure 1. Next we will discuss how estimating the unknown functions



248  $f, g, h$  within this model. Goodness-of-fit of this model is also discussed in  
 249 Section 3.4.

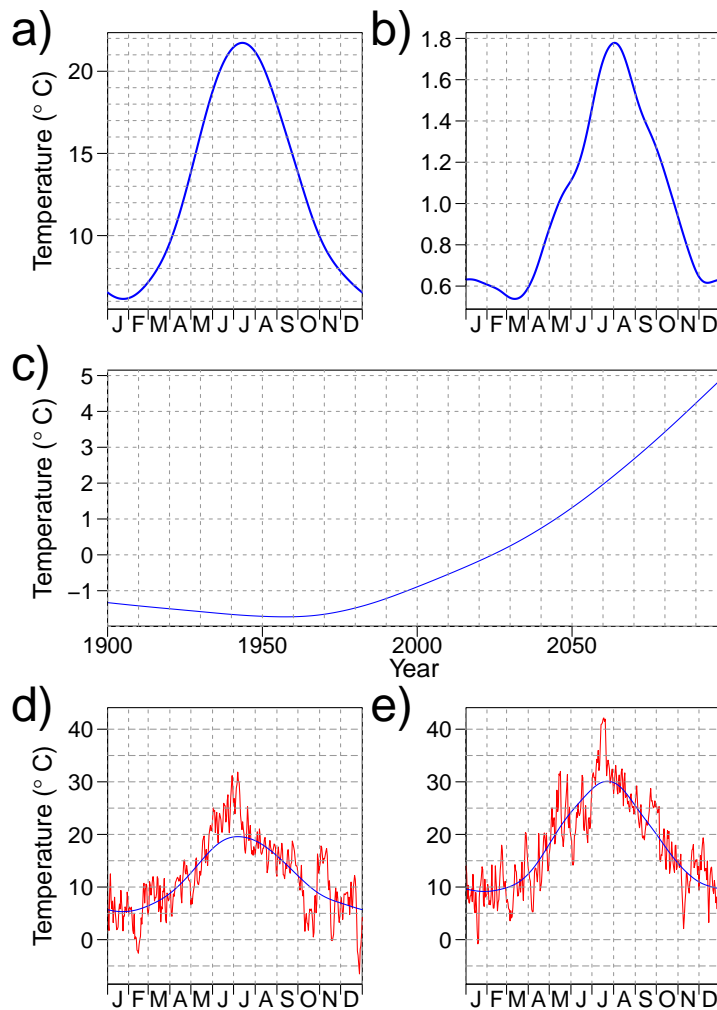


**Fig. 1** Decomposition of a time series (Paris) by the spline model (9). a) represents the reference seasonal cycle  $f$  with  $df=11$  (see section 2.4), b) illustrates the seasonal drift  $h$  with  $df=10$ , and c) represents the annual trend  $g$  with  $df=10$ . The plots d) and e) show the estimation of the annual cycle in 1900 and 2030 respectively. Raw data are shown in red, while the fit of model (1) is in blue.

### 3.2 Estimation Algorithm

Our estimation procedure is a sequential, two-step procedure. Firstly,  $g()$  is estimated using annual mean data only. Secondly,  $f()$  and  $h()$  are estimated assuming that  $g()$  is known.

Both steps involve smoothing with cubic splines. For instance, denoting  $T_{.y} = \frac{1}{365} \sum_{d=1}^{365} T_{d,y}$  the annual mean temperature of year  $y$ , the smoothing splines estimate that  $\hat{g}()$  of  $g()$  can be defined as

$$\hat{g}() = \operatorname{argmin}_{s()} \sum_{i=1}^n (T_{.y} - s(y))^2 + \lambda \int_1^n (s''(x))^2 dx, \quad (10)$$

where the minimum is taken over all possible function  $s()$  belonging to the associated Sobolev space. A spline estimate thus performs a trade-off between closeness to input data (here  $T_{.y}$ ), and roughness (last term in the right-hand side).  $\lambda$  is a regularization parameter determining the level of smoothness. The selection of  $\lambda$  is a common but difficult problem which is addressed in detail in Subsection 3.3. Remarkably, the solutions of (10) are known in closed forms and can be computed easily.

Furthermore, we attempt to provide a calculation which meets operational constraints, and which is thus computationally not too expensive so as to apply it to multiple grid points. For this reason we implemented the sequential algorithm described below.

---

#### Algorithm

---

##### 1 Estimation of $g()$ :

Calculate the annual means  $T_{.y}$ . From the  $T_{.y}$  time-series, compute the smoothing spline estimate  $\hat{g}()$  of  $g()$ , with a given  $df_g$ . Note that this estimate has to be centered subsequently in order to satisfy the identifiability constrains.

##### 2 Linear regression on $\hat{g}(y)$ :

For each day  $d \in \llbracket 1, 365 \rrbracket$ , the time-series  $T_{y,d}$  is linearly regressed onto  $\hat{g}(y)$ , i.e. we estimate the coefficients  $\alpha_d, \beta_d$  involved in:

$$T_{d,y} = \alpha_d + \hat{g}(y)\beta_d + \varepsilon_{y,d}. \quad (11)$$

Thanks to orthogonality,  $\hat{\alpha}_d = T_{d,.}$ , where  $T_{d.} = \frac{1}{n} \sum_{y=1}^n T_{y,d}$ , and  $\hat{\beta}_d = \frac{\sum_{y=1}^n \hat{g}(y)T_{d,y}}{\sum_{y=1}^n \hat{g}(y)^2}$ .

##### 3 Estimation of $f()$ and $h()$ :

From the series  $\hat{\alpha}_d$  and  $\hat{\beta}_d$ , respectively, we calculate the estimates  $\hat{f}()$  and  $\hat{h}()$ , as periodic cubic smoothing splines estimates, with given  $df_f$  and  $df_h$ .

---

As it is sequential and based on an orthogonal design in the regression step, this algorithm is very rapid. A more sophisticated, iterated version of the algorithm has also been studied, and is presented in Appendix C. This variant showed no real improvement however and was thus dismissed.

Predictions based on the model (9) can be derived by extrapolating the estimated spline  $\hat{g}()$  to the year in question. Note that, as natural splines are used to estimate  $g$  (i.e second derivatives are null at the terminating points), this extrapolation is linear.

### 3.3 Selecting degrees of freedom

The selection of the smoothing parameters  $\lambda$  (there is one parameter for each function  $f()$ ,  $g()$  and  $h()$ ), will be discussed in terms of "equivalent degrees of freedom" ( $df$ ), as in many spline papers.  $df$  is meant to be the equivalent of the number of parametric predictors involved in the estimation of the function. The smaller the  $df$ , the smoother the function estimate. Note that  $df$  is a complex one-to-one function of  $\lambda$  – but this correspondence will not be detailed further.

The determination of the different degrees of freedom ( $df$ ) is performed using a variant of cross validation methods adapted to a prediction context. We use a multi-model ensemble of transient simulations covering the 1850-2100 period (see Section 2.1) as plausible realizations of the real world. From this dataset, we look for the value of  $df$  allowing the best prediction for the coming decade (e.g. 2011-2020) using data from previous years (e.g. 1850-2010).

This procedure is distinct from common cross-validation. Usual cross-validation would, in our case, consist of removing one or several years from the available observations (e.g. 1850-2017 if we are in 2018), and tuning the  $df$  coefficients to make the estimated normals as close as possible to the years removed. This procedure is then repeated by removing different years. If this type of cross-validation were used, then the  $df$  coefficients would be optimized to best estimate normals in the past – a period over which climate exhibits no or little change. Given that the non-stationary feature of climate is larger now than in the past, the best  $df$  for prediction might differ from the best  $df$  in the past – we checked that this was effectively the case.

Finally, the three coefficients involved, hereafter  $df_f$ ,  $df_g$ ,  $df_h$ , are estimated sequentially, instead of simultaneously. This makes the selection procedure computationally more affordable.

In each of the three cases, the observation is decomposed into a training sample and a testing sample. For various values of the number of degrees of freedom  $df$ , the considered function ( $f$ ,  $g$  or  $h$ ) is estimated on the training sample and then compared to the testing sample by measuring a Mean Square Error (MSE). Results are averaged over the available climate models. The  $df$  leading to the smallest MSE is then selected. In addition to the MSE value, we estimate its standard deviation which enables the computation of a plausible range of values for  $df$ , through the *one standard error rule* Hastie, Tibshirani, and Wainwright (2015).

329 *Degree of freedom of the reference cycle  $f()$* 

330  $f()$  is meant to represent the mean annual cycle in a stationary climate. In  
 331 order to select  $df_f$ , we took the periods 1900-1930 as a training sample, and  
 332 1931-1940 as a testing sample. This somewhat subjective choice was motivated  
 333 by the fact that climate in the early 20th century is almost stationary.

334 The selected  $df_f$  is typically between 10 and 20, depending on the loca-  
 335 tion considered. Note that the signal-to-noise ratio is much higher for this  
 336 stationary component  $f()$  than for the remaining  $g()$  and  $h()$  functions, which  
 337 explains why  $df_f$  is relatively large and well defined.

338 *Degree of freedom of the annual trend  $g()$* 

339 Unlike  $df_f$ ,  $df_g$  depends on the decade considered. For a given decade  $D$  (for  
 340 example 2001-2010), we use the data prior to  $D$  (i.e. the period 1862-2000) as  
 341 a training sample, the decade itself being the testing sample. Again, we use  
 342 the *one standard error rule* to assess a range of value for  $df_g$ .

343 Our selection procedure for  $df_g$  is illustrated in Figure 2a–b. Note that  
 344 only annual mean values are used there. Focusing on the 2050 decade, the  
 345 best value for  $df_g$  lies between 5 and 6 (panel a). Values smaller than 3 are  
 346 clearly discarded, but the accuracy of the estimated normals is only slightly  
 347 deteriorated if larger  $df_g$  are used (up to more than 15). Remarkably, the  
 348 selected  $df_g$  is almost constant from 1990 to 2100 (panel b), with optimal values  
 349 around 6. This applies to many other locations (not shown). Moreover, as the  
 350 cross validation curve was very flat around its minimum, for all predictions  
 351 made after 1990, we will use  $df_g = 6$  in the following. Using such a constant  
 352 value makes the algorithm easier to implement.

353 *Degree of freedom of the delta cycle  $h()$* 

354 Once  $df_f$  and  $df_g$  have been determined, estimates of  $f()$  and  $g()$  can be  
 355 derived, and  $df_h$  is the only missing parameter to fit. In order to select  $df_h$   
 356 for a given year (2018 for example), we used *the past* (i.e. 1862–2017) as a  
 357 training sample, then calculate the mean square error (MSE) over the next  
 358 year (2018 in this case). Due to the strength of internal variability, we applied  
 359 a smoothing over time. For each year, the selected  $df_h$  is the one minimising  
 360 the smoothed MSE (see Figure 2c–d).

361 Our results suggest that  $df_h$  is the most sensitive (and therefore difficult  
 362 to estimate) parameter in our statistical model. The selected values for  $df_h$   
 363 vary substantially both over space and time. In the case of Paris (Figure 2d),  
 364  $df_h$  increases with time from near 1 (i.e. the minimum possible value, corre-  
 365 sponding to no change in the annual cycle) to 10 in 2100. This corresponds  
 366 to the signal-to-noise increase across the 21st century. In 1990, climate change  
 367 was limited, and it is unclear which season experienced the greatest warm-  
 368 ing. It is thus safer to assume a flat response (i.e. the same degree of warming

369 throughout the year). During subsequent decades, this changing signal (including  
 370 change in the annual cycle) becomes clearer and greater flexibility in  $h()$   
 371 becomes effective.

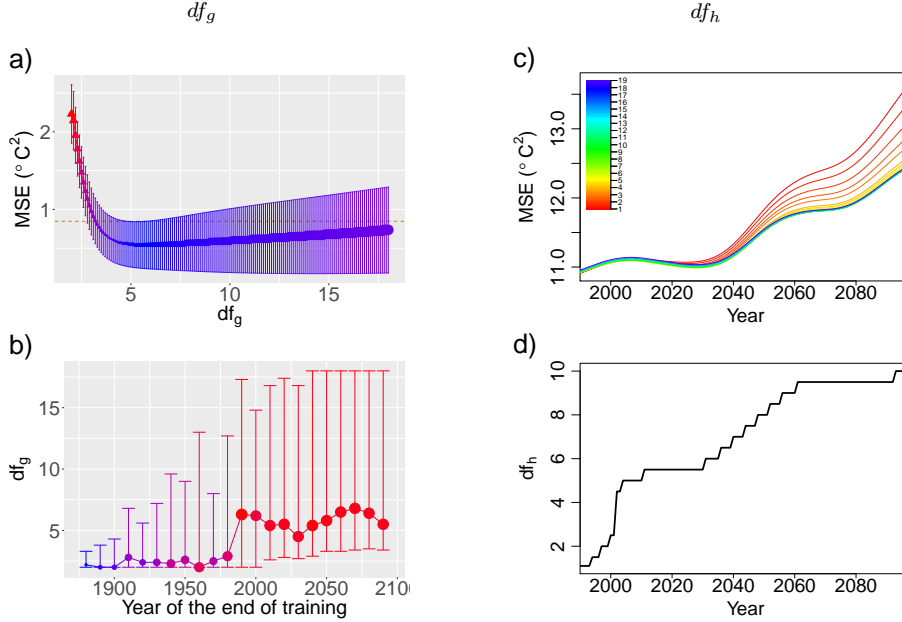


**Fig. 2** Selecting  $df_g$  and  $df_h$ . **a)** error of annual mean temperature normals (points) for the decade 2050 (normals are estimated from 1862-2050 data, error is calculated over 2051-2060), and its standard deviation (bars), as a function of  $df_g$ . **b)** selected  $df_g$  (points), with the corresponding uncertainty according to the one standard error rule (bars), as a function of the predicted decade  $D$ . **c)** Mean square prediction error of daily normals as a function of time, for different values of  $df_h$  ( $df_g, df_f$  are given). **d)** Selected  $df_h$  as a function of the predicted year. All calculations in this figure are made for the Paris (France) grid-point.

### 372 3.4 Model goodness-of-fit

373 An important step in order to validate the use of our statistical model (9)  
 374 and its underlying assumption is to assess the goodness-of-fit to this model.  
 375 This can be done using climate model data, and fitting the model across the  
 376 entire period considered (1862–2100). Such diagnoses are shown in Figure 3.  
 377 Consistent with Figure 1, these diagnoses apply to Paris and the CNRM-CM5  
 378 climate model; they are representative of different locations and models.

379 Firstly, the determination coefficient  $R^2 = 0.73$  is relatively high, and  
 380 consistent with the internal climate variability. Residuals show no abnormal  
 381 patterns: the Gaussian assumption is reasonably well-satisfied (2a), and they

do not exhibit clear dependence on the fitted value (2b). Note that in the latter panel, the density of points depend strongly on the fitted values, thanks to the annual cycle and the fact that the climate is almost stationary over the first 100 years. For instance, the accumulation around  $19^{\circ}\text{C}$  is due to pre-industrial summer maxima.

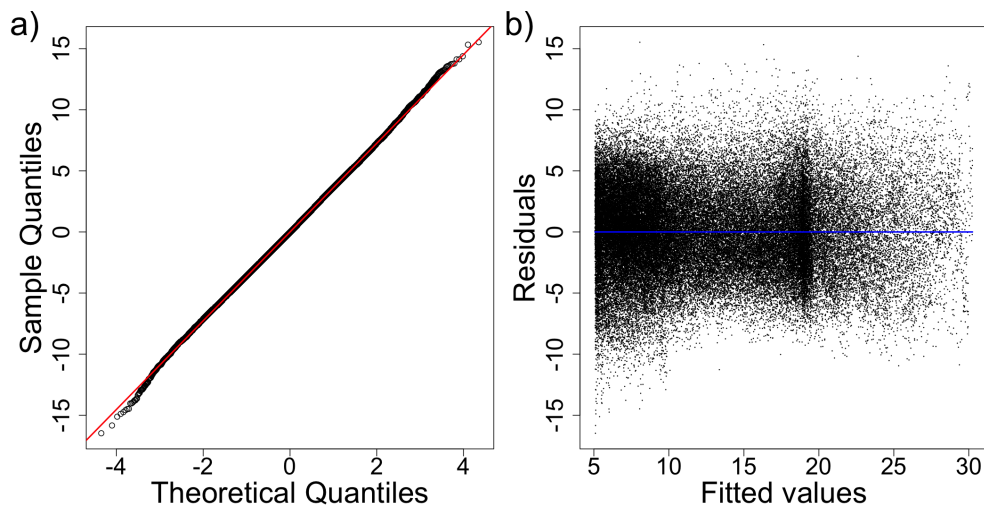


**Fig. 3** Goodness-of-fit to our statistical model. **a)** normal QQ-plot of the residuals. **b)** residual vs fitted values plot.

## 4 Results

### 4.1 Scores on annual mean temperature

The results of the five methods introduced above are compared for annual mean temperatures in Figure 4. The comparison is performed for 4 distinct locations, corresponding to different climates (mean temperature ranges from  $-32^{\circ}\text{C}$  to  $+27^{\circ}\text{C}$ ), amounts of warming (from  $4^{\circ}\text{C}$  to  $8^{\circ}\text{C}$  in 2100 under RCP8.5), and signal-to-noise ratio (internal variability being relatively smaller in the tropics).

Globally, for all locations, the methods have almost the same performance until the late 20th century (near 1990 or 2000, depending on the location). The hinge fit however seems to exhibit a larger variance after 1975 (see e.g. quick variations in Alert and Bengaluru). This is because very few points contribute significantly to fit the broken line's trend. This also applies to a lesser extent to OCN, given that the average is calculated on a smaller number of years than that of the WMO. The sampling margin of error is therefore larger.

402 During the early 21st century, methods based on averaging over past years  
 403 (namely OCN, WMO, and WMO reset), are starting to depart from the refer-  
 404 ence, and show a negative bias. Hinge fit and our technique do a much better  
 405 job and remain close to the reference.

406 Lastly, our method performs much better than any other in the second  
 407 half of the 21st century. While this method remains continuously close to the  
 408 reference, alternatives systematically underestimate the current state of the  
 409 climate, by .5 to 1 degree.

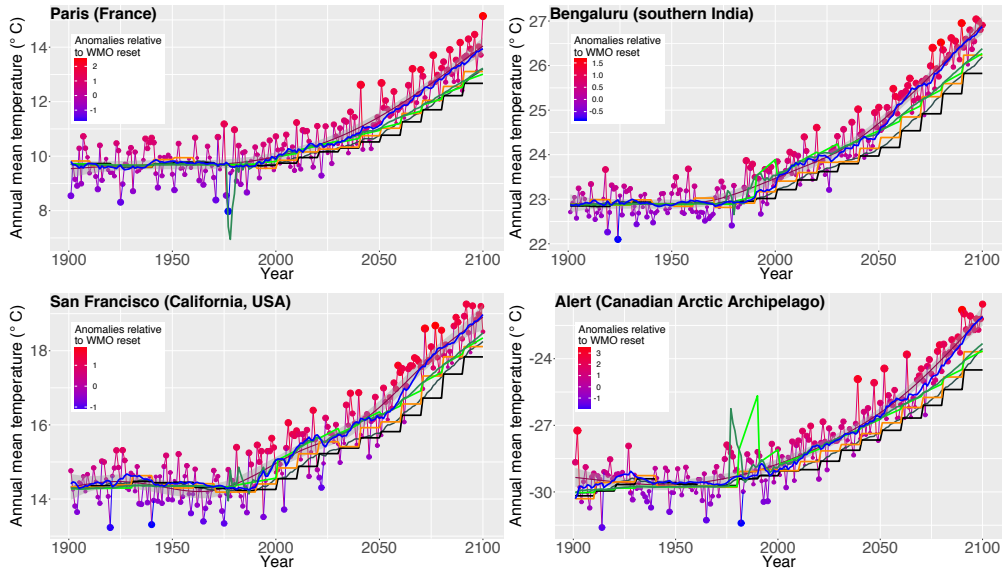


**Fig. 4** Annual mean temperature and estimated normals. Temperature normals on an RCP8.5 scenario of the CNRM-CM5 model. Time-series of annual mean temperature (points) at four different locations (panels). Climatological normals are estimated using 6 different techniques: WMO standard (black line), WMO reset (grey), OCN (yellow), hinge fit (light green), hinge fit reset (dark green), and our method (blue). Normals for a given year (e.g. 2018) are estimated using data from previous years (e.g. 1900-2017). A smoothing spline of the entire time-series (1900-2100; purple line) can be considered as a reference. Anomalies of individual years are calculated with respect to the WMO reset, in order to further illustrate the bias related to this method. All calculations are based on one RCP8.5 simulation from CNRM-CM5.

410 Beyond the illustrative and qualitative assessment made in Figure 4, meth-  
 411 ods can be quantitatively compared using standard criterion such as MSE, bias  
 412 and variance. Such a score-based comparison will be carried out in detail in  
 413 the next section for daily normals. It is also appropriate on annual time-scales,  
 414 and is illustrated in appendix. These quantitative results are consistent with  
 415 those described above.

## 416 4.2 Scores on the daily timescale

417 Figure 5 compares the performance of the 5 considered methods, at the daily  
418 timescale, and for one grid point near San Francisco. Again, the estimation  
419 techniques are trained on all years prior to the one predicted, then the esti-  
420 mated normals are extrapolated to that year. Evaluation of the methods is  
421 based primarily on the mean square error (MSE)(Council et al, 2010). The  
422 latter is also decomposed as the sum of the  $bias^2$  and the variance.

423 Bias varies from 0 to more than  $1^\circ\text{C}$  depending on the method and period  
424 of time. If all methods are nearly unbiased in the late 20th century, only our  
425 approach remains unbiased throughout the 21st century. Alternatives exhibit  
426 negative bias as large as .5 to  $.8^\circ\text{C}$ , except for the standard WMO approach  
427 for which the bias is even larger, near or beyond  $1^\circ\text{C}$ . Even though hinge and  
428 hinge reset lie close to our method until 2040, their bias are slightly larger,  
429 on average. Overall, in the 2000-2100 period, methods can be sorted with re-  
430 spect to their bias (increasing order): our method, hinge reset, hinge, OCN,  
431 and WMO. These results are highly consistent with those obtained on annual  
432 mean temperature.

433  
434 The variance of all estimation techniques are in fact very close to one an-  
435 other. Only the hinge and hinge reset estimators yield a slightly higher variance  
436 than others, especially near the beginning of the period. Our technique has  
437 the lowest variance on average over the entire period.

438 In terms of Mean Square Error (MSE), which is an aggregation of bias and  
439 variance and a very usual criterion, our technique performs much better than  
440 all proposed alternatives. OCN and WMO approaches are reasonably accurate  
441 near the beginning of the period, for instance before 2020, when climate change  
442 remains slight. They are penalized by their large bias subsequently. The two  
443 variants of the hinge technique suffer from their large variance at the beginning,  
444 then rank second from 2010 to 2020.

445 Two additional remarks can be made. Firstly, results found for other loca-  
446 tions were qualitatively similar. In particular, they confirm that our method  
447 outperforms the proposed alternatives, and remains almost unbiased across  
448 the 21st century. Secondly, all methods reset on a decadal basis exhibit some  
449 degradation of their scores at the end of each decade (WMO, OCN and hinge).  
450 This is particularly pronounced in the bias of OCN and WMO.

451 Overall, these results suggest that our method is more accurate than ex-  
452 isting alternatives. This happens both in terms of bias and variance, which  
453 can be underlined. Furthermore, very low bias is revealed over the 21st cen-  
454 tury. This suggests that our technique has the appropriate level of flexibility  
455 to follow climate change, whilst not having too much variance. As our method  
456 exhibits almost no bias, potentially more sophisticated methods could improve  
457 on the variance (the bias is already minimal). This would probably lead to lim-  
458 ited gain in terms of total MSE, as a large part of this variance is related to  
459 (irreducible) internal climate variability.



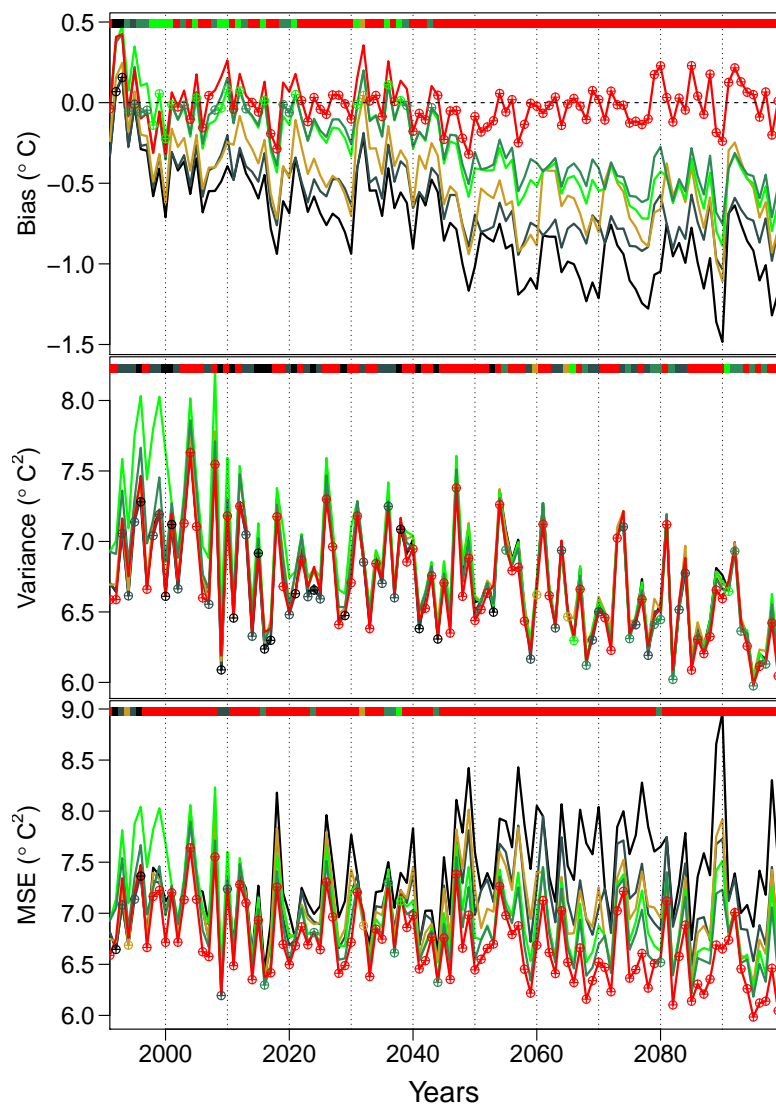


**Fig. 5** Daily scores in San Francisco. Six techniques for estimating daily normals, namely WMO standard (black), WMO reset (grey), OCN (yellow), hinge fit (light green), hinge fit reset (dark green), and our method (red), are compared. Their evaluation is based on their bias (top), variance (middle), and mean square error (MSE, bottom). The year in the  $x$ -axis denotes the end of the training period; prediction is made for the following year. The coloured line (top of each panels) indicates which method performs best, for a given criterion and a given year. Calculations are made for one grid-point near San Francisco, using an ensemble of RCP8.5 simulation from the CMIP5 archive.

## 5 Conclusion and discussion

In this paper, we introduce a new method for estimating daily climatological normals, describing the corresponding model. This technique relies on the assumption that the response to climate change is smooth over time and nears the pattern scaling assumption. All terms can be estimated using smoothing splines. The proposed estimation algorithm is very fast and this is due to a two-step (as opposed to simultaneous) procedure. The main challenge is the tuning of the smoothing parameters which is done using an extension of cross validation specifically designed for prediction.

Our method is compared to previously proposed alternatives in a predictive sense: methods are used to estimate climatological normals for the next, unobserved year. Their accuracy is compared on that basis, using an ensemble of RCP8.5 simulation from the CMIP5 ensemble in a perfect model framework.

Results show that our method is more accurate than all considered alternatives on the yearly timescale. The gap is particularly large across the second part of the 21<sup>st</sup> century. Additionally, on the daily timescale, our method was also shown to provide the best results in terms of bias, variance, and therefore mean square error. These good properties can be partly attributed to the flexibility of the method, adjusted through the selection of smoothing parameters.

Our results thus suggest that the proposed method brings a strong improvement in the estimation of climatological normals accounting for climate change. Such revised – with respect to the WMO recommendation – normals could be used to address several questions. Unbiased normals could be particularly useful for climate monitoring, e.g. qualify if a year or season is warmer or colder than *really* expected. It could also be used to produce climate change corrected time-series. This would be relevant e.g. to compare how anomalous different years or periods are. As a typical illustration, one might wonder if an extreme event like the 2003 European Event remains unprecedented after correction for the climate change effect. Additionally, our method could be used to provide a refined description of on-going climate change with respect to the annual cycle, i.e. beyond the annual mean warming.

These attractive features do not mean that the standard way of computing climatological normals is now obsolete. Having a stationary reference such as the WMO standard is still very valuable, e.g. in order to highlight climate change. We suggest therefore that weather or climate services in charge of climate monitoring could compute two different sets of normals – a stationary reference and a climate change corrected set of normals – and use one or the other depending on the application considered. Updating the revised set of normals on a regular annual basis seems to be something required for the delivery of an estimation as accurate as possible.

Future work on the method described in this paper could include the estimation of uncertainties in the estimated normals. This would be very valuable, e.g. for assessing the uncertainties in climate change corrected time-series. Future work could also include a pre-computation of smoothing parameters for a large number of locations, in order to make the method even easier to imple-

---

505 ment. This tuning step remains the most difficult in our procedure and has to  
506 be re-examined carefully for different places. Lastly, the selection of smoothing  
507 parameters could be re-examined for different emission scenarios for the shape  
508 of the time response (and therefore the optimal value of smoothing parame-  
509 ters) greatly depends on the emission pathway.

## Appendix

The analysis in this article has been performed using the statistical software R.

### A Computational and simulation details

The 21 simulations used for daily mean temperature were:

ACCESS1-0, ACCESS1-3, CCSM4, CESM1-BGC, CMCC-CMS, CNRM-CM5, CSIRO-Mk3-6-0, CanESM2, GFDL-CM3, GFDL-ESM2G, GFDL-ESM2M, IPSL-CM5A-LR, IPSL-CM5A-MR, IPSL-CM5B-LR, MIROC-ESM-CHEM, MIROC-ESM, MPI-ESM-LR, MPI-ESM-MR, MRI-CGCM3, NorESM1-M, inmcm4

The simulations used for annual mean temperature were:

ACCS0\_r1i1p1, ACCS3\_r1i1p1, BCC1\_r1i1p1, BCCm\_r1i1p1, BNU\_r1i1p1, CCCMA\_r1i1p1, CCCMA\_r2i1p1, CCCMA\_r3i1p1, CCCMA\_r4i1p1, CCCMA\_r5i1p1, CNRM\_r10i1p1, CNRM\_r1i1p1, CNRM\_r2i1p1, CNRM\_r4i1p1, CNRM\_r6i1p1, CSIRO\_r10i1p1, CSIRO\_r1i1p1, CSIRO\_r2i1p1, CSIRO\_r3i1p1, CSIRO\_r4i1p1, CSIRO\_r5i1p1, CSIRO\_r6i1p1, CSIRO\_r7i1p1, CSIRO\_r8i1p1, CSIRO\_r9i1p1, GFDLc\_r1i1p1, GFDLg\_r1i1p1, GFDLm\_r1i1p1, GISSr\_r1i1p1, IAPg\_r1i1p1, IAPs\_r1i1p1, IAPs\_r2i1p1, IAPs\_r3i1p1, INGVc\_r1i1p1, INGVe\_r1i1p1, INGVs\_r1i1p1, INM\_r1i1p1, IPSLal\_r1i1p1, IPSLal\_r2i1p1, IPSLal\_r3i1p1, IPSLal\_r4i1p1, IPSLam\_r1i1p1, IPSLb\_r1i1p1, MIROC5\_r1i1p1, MIROC5\_r2i1p1, MIROC5\_r3i1p1, MIROCC\_r1i1p1, MIROCCe\_r1i1p1, MPIMl\_r1i1p1, MPIMl\_r2i1p1, MPIMl\_r3i1p1, MPIMm\_r1i1p1, MRI\_r1i1p1, NCARc\_r1i1p1, NCARc\_r2i1p1, NCARc\_r3i1p1, NCARc\_r4i1p1, NCARc\_r5i1p1, NCARc\_r6i1p1, NCARE\_r1i1p1

### B Another system of constraints for model (9)

Once we have obtained the decomposition of model (9), it is possible to make it more interpretable. Let  $\tilde{g} = g - g(1)$ ,  $\tilde{f} = f + g(1).h$ . Then, the decomposition of model (1) can be rewritten as:

$$\begin{aligned} f(d) + g(y).h(d) &= (f(d) + g(1).h(d)) + (g(y) - g(1)).h(d) \\ &= \tilde{f}(d) + \tilde{g}(y).h(d) \end{aligned}$$

Thus,  $\tilde{f}$  represents the annual reference cycle of the first year of the considered period and  $\tilde{g}$  quantifies the annual mean temperature evolution. Therefore the first value,  $\tilde{g}(1)$ , is zero.

541 **C Alternating least squares**

542 Addition of a few steps to the sequential algorithm permitting an iter-  
543 ative procedure:

544 **4 Re-estimation of  $g()$ :**

545 We now fix  $\hat{f}, \hat{h}$  and estimate  $g$  once again, the goal of the procedure  
546 being minimization of the total sum of squares

547 i.e  $RSS = \sum_{y,d} (T_{y,d} - \hat{f}_d - \hat{g}_y \cdot \hat{h}_d)^2$ .

548 For a fixed  $y$ , let us define:

549  $RSS_y = \sum_d ((T_{y,d} - \hat{f}_d) - g_y \cdot \hat{h}_d)^2 = \sum_d (\tilde{T}_{y,d} - g_y \cdot \hat{h}_d)^2$

550 where  $\tilde{T}_{y,d} = T_{y,d} - \hat{f}_d$

551 let  $g_{0,y}$  the mean square estimator  $g_{0,y} = \frac{\sum_{j=1}^{365} \hat{h}_d \cdot T_{y,d}}{\sum_{j=1}^{365} \hat{h}_d^2}$

552 Also by the Pythagorean theorem:

553

$$\begin{aligned} \sum_{d=1}^{365} (\tilde{T}_{y,d} - g_y \cdot \hat{h}_d)^2 &= \sum_{d=1}^{365} (\tilde{T}_{y,d} - g_{0,y} \cdot \hat{h}_d + (g_{0,y} - g_y) \cdot \hat{h}_d)^2 \\ &= \sum_{d=1}^{365} (\tilde{T}_{y,d} - g_{0,y} \cdot \hat{h}_d)^2 + \sum_{d=1}^{365} ((g_{0,y} - g_y) \cdot \hat{h}_d)^2 \\ &= \sum_{d=1}^{365} (\tilde{T}_{y,d} - g_{0,y} \cdot \hat{h}_d)^2 + (g_{0,y} - g_y)^2 \cdot \sum_{d=1}^{365} \hat{h}_d^2 \end{aligned}$$

Finally,

$$\begin{aligned} RSS &= \sum_{y=1}^n RSS_y \\ &= \sum_{d,y} (\tilde{T}_{y,d} - g_{0,y} \cdot \hat{h}_d)^2 + \sum_{y=1}^n (g_{0,y} - g_y)^2 \cdot \sum_{d=1}^{365} \hat{h}_d^2 \end{aligned}$$

554 Then, we compute the smoothing spline estimate  $\hat{g}()$  of  $g_{0,y}$ , with  
555 the given  $df_g$ .

556 5 We iterate steps 3 and 4 to minimize sum of squares  $RSS$ .

557 **D Annual scoring for normals**

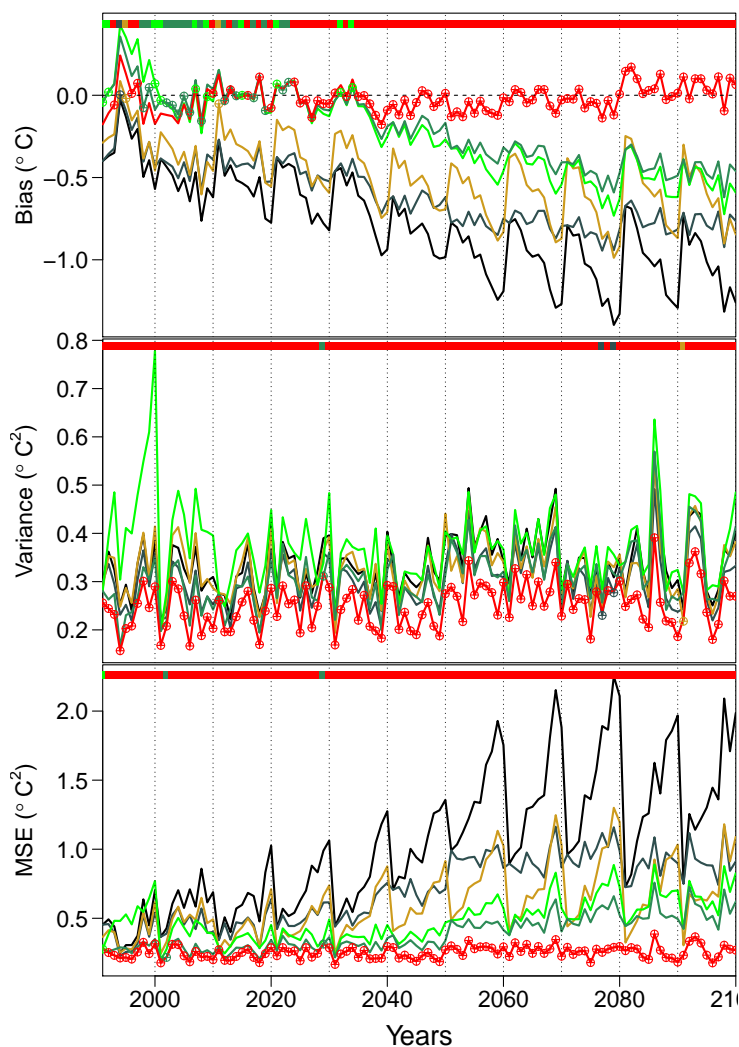


**Fig. 6** The three plots illustrate scoring on the yearly mean temperature at San Francisco, for each year normal prediction occurs on all CMIP5 models. The horizontal axis represents the end of the training period and for each method, prediction occurs the following year. The upper line shows, for each score, the winning method for predicting the next year. The different calculations are WMO (black), WMO reset (grey), OCN (yellow), hinge (light green), hinge fit reset (green) and model(9) (blue). The upper figure shows the evolution of the bias, the middle one represents the variance of the prediction and the bottom plot illustrates the evolution of the mean square prediction error (MSE).

558 **Acknowledgements** The authors acknowledge Météo-France for supporting this study. They  
559 also wish to thank the climate modeling groups involved in CMIP5 for producing and sharing  
560 their simulations.

## 561 References

- 562 Arguez A, Applequist S (2013) A harmonic approach for cal-  
563 culating daily temperature normals constrained by homoge-  
564 nized monthly temperature normals. *Journal of Atmospheric*  
565 *and Oceanic Technology* 30(7):1259–1265, DOI 10.1175/JTECH-  
566 D-12-00195.1, URL <https://doi.org/10.1175/JTECH-D-12-00195.1>,  
567 <https://doi.org/10.1175/JTECH-D-12-00195.1>
- 568 Arguez A, Vose RS (2011) The definition of the standard  
569 WMO climate normal: The key to deriving alternative cli-  
570 mate normals. *Bulletin of the American Meteorological Soci-*  
571 *ety* 92(6):699–704, DOI 10.1175/2010BAMS2955.1, URL  
572 <http://journals.ametsoc.org/doi/pdf/10.1175/2010BAMS2955.1>
- 573 Arguez A, Applequist S, Vose RS, Durre I, Squires MF,  
574 Yin X (2011) NOAA’s 1981–2010 climate normals:  
575 Methodology of temperature-related normals. Tech. rep.,  
576 URL [https://www1.ncdc.noaa.gov/pub/data/normals/1981-](https://www1.ncdc.noaa.gov/pub/data/normals/1981-2010/documentation/temperature-methodology.pdf)  
577 [2010/documentation/temperature-methodology.pdf](https://www1.ncdc.noaa.gov/pub/data/normals/1981-2010/documentation/temperature-methodology.pdf)
- 578 Arguez A, Durre I, Applequist S, Vose RS, Squires MF, Yin X, Heim  
579 RR, Owen TW (2012) NOAA’s 1981–2010 U.S. climate normals. *Bul-*  
580 *letin of the American Meteorological Society* 93(11):1687–1697, DOI  
581 10.1175/BAMS-D-11-00197.1
- 582 Arguez A, Vose RS, Dissen J (2013) Alternative climate normals: Im-  
583 pacts to the energy industry. In: *Bulletin of the American Mete-*  
584 *orological Society*, vol 94, pp 915–917, DOI 10.1175/BAMS-D-12-  
585 00155.1, URL [http://journals.ametsoc.org/doi/pdf/10.1175/BAMS-](http://journals.ametsoc.org/doi/pdf/10.1175/BAMS-D-12-00155.1)  
586 [D-12-00155.1](http://journals.ametsoc.org/doi/pdf/10.1175/BAMS-D-12-00155.1)
- 587 Azaïs JM, Ribes A (2016) Multivariate spline analy-  
588 sis for multiplicative models: Estimation, testing and  
589 application to climate change. *Journal of Multivariate*  
590 *Analysis* 144:38–53, DOI 10.1016/j.jmva.2015.09.026,  
591 URL [http://ac.els-cdn.com/S0047259X15002560/1-s2.0-](http://ac.els-cdn.com/S0047259X15002560/1-s2.0-S0047259X15002560-main.pdf?_tid=b6d26b82-243a-11e7-95bb-00000aacb362&acdnat=1492522205_708816799da1e435d00bab291f7a5631)  
592 [S0047259X15002560-main.pdf?\\_tid=b6d26b82-243a-11e7-95bb-](http://ac.els-cdn.com/S0047259X15002560/1-s2.0-S0047259X15002560-main.pdf?_tid=b6d26b82-243a-11e7-95bb-00000aacb362&acdnat=1492522205_708816799da1e435d00bab291f7a5631)  
593 [00000aacb362&acdnat=1492522205\\_708816799da1e435d00bab291f7a5631](http://ac.els-cdn.com/S0047259X15002560/1-s2.0-S0047259X15002560-main.pdf?_tid=b6d26b82-243a-11e7-95bb-00000aacb362&acdnat=1492522205_708816799da1e435d00bab291f7a5631)
- 594 Baddour O (2011) Climate Normals, World Mete-  
595 orological Organization Commission for Climatol-  
596 ogy Management Group Meeting , ITEM 10 URL  
597 [http://www.wmo.int/pages/prog/wcp/ccl/mg/documents/mg2011/CCl-](http://www.wmo.int/pages/prog/wcp/ccl/mg/documents/mg2011/CCl-MG-2011-Doc_10_climatnormals1.pdf)  
598 [MG-2011-Doc\\_10\\_climatnormals1.pdf](http://www.wmo.int/pages/prog/wcp/ccl/mg/documents/mg2011/CCl-MG-2011-Doc_10_climatnormals1.pdf)
- 599 Council NR, et al (2010) Assessment of intraseasonal to interannual  
600 climate prediction and predictability. National Academies Press

- 601 Geoffroy O, Saint-Martin D (2014) Pattern decomposition of the tran-  
602 sient climate response 66:23,393
- 603 Hastie T, Tibshirani R, Wainwright M (2015) Statistical learning with  
604 sparsity: the lasso and generalizations. CRC press
- 605 Huang J, van den Dool HM, Barnston AG (1996) Long-lead seasonal  
606 temperature prediction using optimal climate normals. *Journal of Cli-*  
607 *mate* 9(4):809–817
- 608 Krakauer NY (2012) Estimating climate trends: Application to united  
609 states plant hardiness zones. *Advances in Meteorology* DOI  
610 10.1155/2012/404876
- 611 Krakauer NY, Devineni N (2015) Up-to-date probabilistic  
612 temperature climatologies. *Environ Res Lett Environ Res*  
613 *Lett* 10(10), DOI 10.1088/1748-9326/10/2/024014, URL  
614 <http://iopscience.iop.org/1748-9326/10/2/024014>
- 615 Livezey RE, Vinnikov KY, Timofeyeva MM, Tinker R, van den  
616 Dool HM (2007) Estimation and extrapolation of climate nor-  
617 mals and climatic trends. *Journal of Applied Meteorology and*  
618 *Climatology* 46(11):1759–1776, DOI 10.1175/2007JAMC1666.1,  
619 URL <https://doi.org/10.1175/2007JAMC1666.1>,  
620 <https://doi.org/10.1175/2007JAMC1666.1>
- 621 Mitchell TD (2003) An Examination of the Accuracy  
622 of the Technique for Describing Future Climates. *Cli-*  
623 *matic Change* Volume 60(Issue 3):pp 217–242, URL  
624 <https://link.springer.com/content/pdf/10.1023%2FA%3A1026035305597.pdf>
- 625 Scherrer SC, Appenzeller C, Liniger MA (2006) Temperature trends in  
626 Switzerland and Europe: Implications for climate normals. *Interna-*  
627 *tional Journal of Climatology* DOI 10.1002/joc.1270
- 628 Tebaldi C, Arblaster J (2014) Pattern scaling: Its strengths and lim-  
629 itations, and an update on the latest model simulations. *Climatic*  
630 *Change* 122:459–471, DOI 10.1007/s10584-013-1032-9
- 631 Vinnikov KY, Robock A, Grody NC, Basist A (2004) Anal-  
632 ysis of diurnal and seasonal cycles and trends in climatic  
633 records with arbitrary observation times. *Geophysical Re-*  
634 *search Letters* 31(6):n/a–n/a, DOI 10.1029/2003GL019196, URL  
635 <http://doi.wiley.com/10.1029/2003GL019196>
- 636 Wilks DS (2013) Projecting ”normals” in a nonstationary climate. *Jour-*  
637 *nal of Applied Meteorology and Climatology* 52(2):289–302, DOI  
638 10.1175/JAMC-D-11-0267.1
- 639 Wilks DS, Livezey RE (2013) Performance of alternative “nor-  
640 mals” for tracking climate changes, using homogenized and  
641 nonhomogenized seasonal u.s. surface temperatures. *Journal of*  
642 *Applied Meteorology and Climatology* 52(8):1677–1687, DOI  
643 10.1175/JAMC-D-13-026.1, URL [https://doi.org/10.1175/JAMC-D-](https://doi.org/10.1175/JAMC-D-13-026.1)  
644 [13-026.1](https://doi.org/10.1175/JAMC-D-13-026.1), <https://doi.org/10.1175/JAMC-D-13-026.1>
- 645 World Meteorological Organization (2007) The Role OF Climatolog-  
646 ical Normals In a Changing Climate. WCDMP-No 61 WMO-TD



---

647 No.1377(World Climate Data and Monitoring Programme), URL  
648 [https://www.wmo.int/datastat/documents/WCDMPNo61\\_1.pdf](https://www.wmo.int/datastat/documents/WCDMPNo61_1.pdf)  
649 Wright W (2014) Discussion paper on the calculation of the standard  
650 climate normals: A proposal for a dual system. World Climate Data  
651 and Monitoring Program, accessed 14